Noise suppression for detection and location of microseismic events using a matched filter

Leo Eisner, David Abbott, William B. Barker, James Lakings and Michael P. Thornton, Microseismic Inc.*

Summary

Detection and location of microseismic events is generally limited by seismic noise and inversion velocity model accuracy. These issues can be overcome by using " a matched filter" in order to stack scattered energy and reduce demands on the accuracy of the inversion velocity model for events with similar mechanisms and nearby locations. We have applied the technique to a surface monitoring dataset of the microseismic events induced by hydraulic fracturing to detect and relatively locate events. We have benchmarked detection and relative location with a direct location technique (PSET® technology).

Introduction

Cross-correlation of a noisy time-series with a known signal is an efficient method for detecting weak signals similar to the known signal. This is known as a matched filter and has been broadly used in both earthquake and prospecting seismology for more than 3 decades.

In earthquake seismology, waveform correlation of strong events with noisy time-series is used to detect weaker events (e.g., Gibbons and Ringdal, 2006, and the citations in this study, Hanafy *et.al.* 2008) and locate the detected events relative to the strong event (e.g. Gibbons *et. al.*, 2007). A similar method is also used in reflection seismology, where a complex source-time function, known as chirp or sweep, is used to deconvolve medium response and reconstruct Green's functions between sources and receivers (Yilmaz and Ozdogan, 1987). These techniques take advantage of decomposing the observed time series into a convolution of source, medium and receiver responses; Deconvolution of any of them from the observed data provides the remaining two responses.

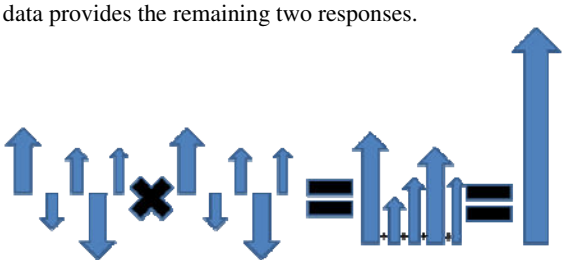

Figure 1: Illustration of noise enhancement by cross-correlation of similar waveforms.

In this study we use the methodology of Gibbons and Ringdal (2006) to detect and relatively locate weak microseismic events induced during hydraulic fracturing as observed by a surface array of vertical component geophones. For the known signal, we are using strong events with signal higher than the noise level at the surface array. The source-time function of these strong events is assumed to be a simple delta function given the size of the microseismic events (up to tens of meters) relative to the distance of the observation points from the source (hundreds to thousands of meters) and the frequency content of the observed signals (10-40 Hz). Thus, both the weak and strong event source-time functions can be approximated by a delta function in time and space and the above outlined methodology will enhance the signal-to-noise ratio of the weak events.

Theory

Arbitrary seismic data observed at any receiver can be described as the convolution of the source, medium and receiver functions (linear elasticity):

$$D(t) = S(t) \otimes G(t) \otimes R(t), \qquad (1)$$

Where t is time, $D(t)$ is seismic data observed (three-components or single component, pressure, etc.), $G(t)$ is medium response (linear sum of Green's functions) and $R(t)$ is receiver function (or receiver response) and $\otimes$ is a convolution in the time domain. Note that the source function $S(t)$ and $G(t)$ are tensors of the second and fourth order and equation (1) represents dyadic product of these two tensors. As explained in the introduction in microseismic monitoring from surface arrays we can assume that the source-time dependency of $S(t)$ is a delta function in time. Furthermore, for nearby events with nearby locations the receiver functions $R(t)$ and path effects $G(t)$ are similar. Finally if the source mechanisms are similar the source excitation S in the equation (1) produces two similar waveforms:

$$\begin{aligned} & D_1(t) = S_1 \bullet G_1(t) \otimes R_1(t) \\ & \cong D_2(t+\tau) = S_2 \bullet G_2(t+\tau) \otimes R_2(t+\tau) \end{aligned}, \qquad (2)$$

Where τ is time delay between events 1 and 2. To take advantage of equation (2) we propose to cross-correlate recordings of a Master event with good signal-to-noise ratio of D_1 with noisy recordings. If an event 2 that satisfies equation (2) is present in such recordings cross-correlation of two similar signals will be high and such event is called a Slave event. However, if the recordings contain only noise or events with different waveforms the cross-correlation remains relatively low. Furthermore, if equation (2) is satisfied, the cross-correlation peaks at exactly the same time on all receivers in our observation array (as the

time delay between the Master and Slave events is the same on all receivers). Thus a high value of stacked cross-correlations from all receivers indicates detection of a Slave event, similar to Master event. Such events are also known as doublets in earthquake seismology.

A cross-correlation of two similar signals enhances the signal-to-noise ratio of the scattered energy as illustrated in Figure 1. The source impulse energy is scattered over a time window by the medium and receiver response (near surface, *G(t)* and *R(t)* in equation (1)). Cross-correlation of Master and Slave events satisfying equation (2) is a sum of squares of the scattered arrivals all contributing to the peak amplitude of the correlation coefficient. However, the microseismic signals are generally not similar to a sweep signal used for vibroseis prospecting, for which the auto-correlation is nearly a delta function. Therefore, the cross-correlation enhancements as illustrated in Figure 1 may produce side-lobes of the correlation function besides the main peak.

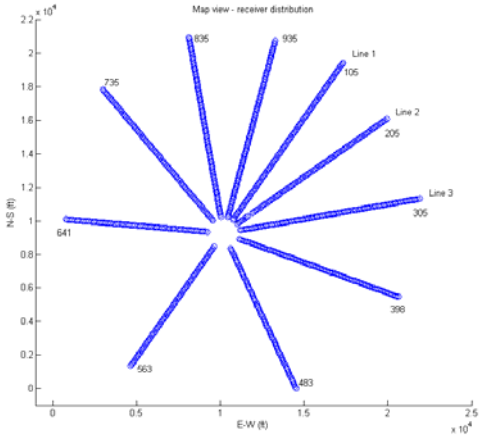

Figure 2 Distribution of surface receivers during monitoring of the hydraulic fracture treatment. The injection pad is approximately in the center of the picture and lines of receivers radiate form the injection pad. The line numbering is indicated for the first three lines and largest number of a receiver in each line is shown.

Application to a real dataset

We have applied the above technique to a dataset from a hydraulic fracture monitoring where the hydraulic fracture was stimulated in several stages of the horizontal treatment well at a depth of approximately 12,000 ft (3,600 m). Six stages of slurry with a proppant were injected into a shale formation. This study investigated the initial 15 minutes of the final sixth stage which reactivated a previously stimulated part of the tight gas reservoir. We were able to detect and locate several hundred events with the stacking of 935 receivers above the reservoir (Lakings *et.al.,* 2005) vicinity of the injection point close to the left most line in Figure 2. Initially, we have observed one strong (Master) event during the first 15 minutes of this fracturing.

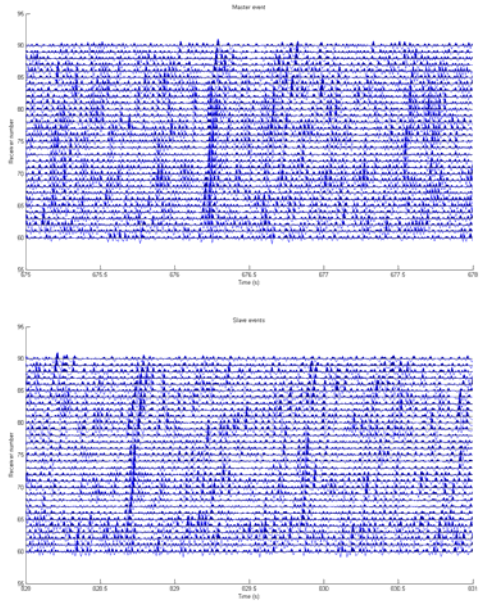

Figure 3 Waveforms of particle velocity on vertical components of line 1 (see Fig. 2) due to the strongest (Master) event detected (around time 767 sec - the top plot) and two weaker (Slave) events (around times 828.5 and 829.7 sec - the lower plot).

Figure 3 shows waveforms processed with noise suppression of the strongest events detected during stage 6 of the previously described hydraulic fracture stimulation. Note that the waveforms show long revibrations probably caused by the path and receiver effects, which last at least 0.4 seconds. Also note that the first arrival is relatively impulsive, indicating a sharp onset of the triggered Master event. The move-out is consistent with a source at approximately the depth of the injection (i.e. 12,000 ft). As the signal-to-noise is relatively good for this event, we use it as the Master event D_1 of equation (2) and cross-correlate a 0.4 second time interval around the Master event with a sliding time intervals from the entire 15 minutes of a dataset recorded during the monitoring. The cross-correlation with zero time-laps is carried between two traces of the Master event and the sliding window at each receiver. However, the cross-correlation with zero time laps is essentially a scalar product of the time vectors between the Master event and data sample.

Figure 4 shows the cross-correlations of the Master event of Figure 3 with 3 seconds of the time windows around the Slave events shown in the lower plot of Figure 4. We show only receivers 50 through 80 of Line 1, where the Master event had a relatively good signal-to-noise ratio (Figure 3).

Note the high correlation for the times around 828.5 and 829.6 seconds. These high cross-correlations correspond to two strong Slave events barely visible in the lower plot of Figure 3. Note that there is virtually no move-out of the peak of the cross-correlations in Figure 4 as the move-outs of Master and Slave events are essentially the same. Let us point out that the cross-correlations shown in Figure 4 removed the move-out without any knowledge of the velocity structure, just by satisfying equation (2). If there is move-out of the Slave events it can be further used to relatively locate as we shall show later.

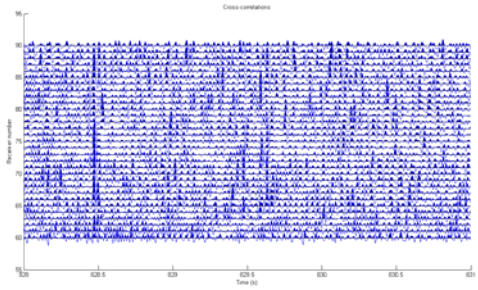

Figure 4 Cross-correlation of the Master and Slave events shown in Figure 3 for receivers 50-80 of line 1 shown in Figure 2.

To find all Slave events which correlate with negligible move-out (negligible relative to the time sampling – 0.004 sec), we have stacked the correlated traces for receivers 1-184 (i.e. most of the receivers in the first two lines) where the Master event had a good signal-to-noise ratio. In Figure 5 we have stacked the entire 15 minute interval of the recorded data. Stacking additional receivers further improves detection of weak events as long as the Master event has a good single-to-noise ratio on these receivers.

Figure 5 reveals the high stack for the Master event at 676 sec. This is not surprising as the autocorrelations stack positively. However, we can also observe high stacks (i.e., highly correlated waveforms on all receivers at the same time) for other Slave events at times 829.632, 828.472 and 727.112 sec. We should keep in mind that Figure 5 shows a simple stack assuming no move-out on stacked receivers. If, however, a Slave event has a different location, we should be stacking along modified move-outs determined from the relative locations of the Master and weak Slave events. For comparison we show also times and amplitudes of the strongest events detected with a direct location technique (PSET®). The amplitudes of the direct locations represent an average energy of the directly stacked events. Unfortunately, the direct location used a different short time window and triggered twice for each of the 4 strongest events. This is because the triggering algorithm falsely detected reflections as new events. If we discard the false triggers we can see that even the simply stacked correlation traces, those without any move-out agree well with the directly located events for the 4 strongest events. Furthermore, the amplitudes of the directly located events are proportional to the signal-to-noise ratio on the stacked (normalized) cross-correlations. The tenth weakest event at 24.5 sec does not correspond to a high stack of correlations even when considering differential move-outs, however, other Slave events detected in this 15 minute monitoring interval correspond to high stacks if relative move-out stacking is applied (not shown in Figure 5).

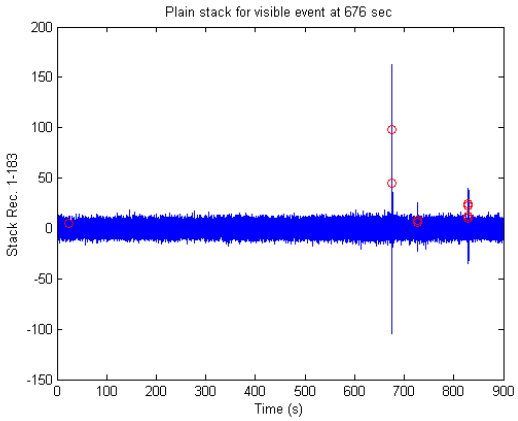

Figure 5 Stacked cross-correlations on receivers 1-183 for 900 sec (15 minutes) of observations. Red circles represent amplitude and origin time of the directly located events (PSET® technology).

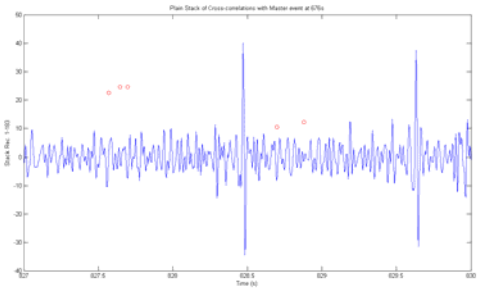

Figure 6 Detail of Figure 5 for times between 827 and 830 sec.

The stacked traces and direct locations for two Slave events at 829.632 and 828.472 sec are shown in Figure 6. The origin times of the direct locations (red circles) precede the stacked traces by approximately 1 sec, which corresponds to the travel-time between the depth of 12,000 ft and the surface. The period of the stacked cross-correlation function is approximately 0.04 sec, corresponding to the dominating frequency of detected signal at 25 Hz.

Figure 7 shows map views of the maxima of correlation stacks for different relative positions of two Slave events from the above dataset. The top map shows well-resolved relative position of the first Slave event in Figure 6

indicating that the Master and Slave events are co-located with an approximate resolution of 100 ft. The lower plot of Figure 7 shows an analogous map for a Slave event detected by the direct location with origin time at 857.5 sec. Although the maximum of the stacked correlations is smaller we can locate this Slave event approximately 200 ft EEN of the Master event.

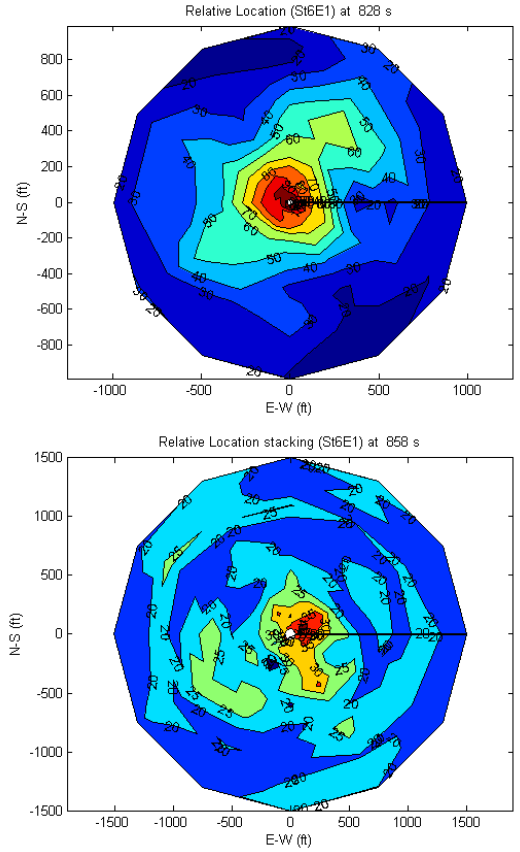

Figure 7 map views of maximum stacks of correlations for relative locations of two Slave events (828 sec at the top plot and 858 sec at the lower plot). The Master event location corresponds to the center of each plot (0,0).

Figure 8 shows three relocated strongest Slave events from Figure 5. The Master event is located south-west of the injection well probably due to an activated natural fracture system. The relatively located Slave events seem to have less scatter and align along E-W trend (within location uncertainty, see Figure 7). The strong Slave events with high signal-to-noise ratio shown in Figure 7 have been relocated by less than 600 ft while weaker Slave events may show larger relocations if PSET and relative locations are compared. Relative locations are probably more accurate as their determination is less sensitive to the velocity model.

Discussion

One may ask why do we observe a large number of Slave events with similar mechanisms in the vicinity of a Master event? Rutledge and Phillips (2003), Eisner *et.al.* (2006) and many others have shown that the hydraulically induced events observed with downhole instruments show a high degree of similarity and nearly uniform pattern of mechanisms. Another reason for the high number of similar events may be due to the possibility that the largest events are associated with large fault. Their smaller aftershocks (or foreshocks or repeated failures) may provide crucial information about the fracture propagation along these structures.

Note that relative location through cross-correlation stacking automatically includes any changes due to source mechanism and all receivers contribute positively to relative location stacking.

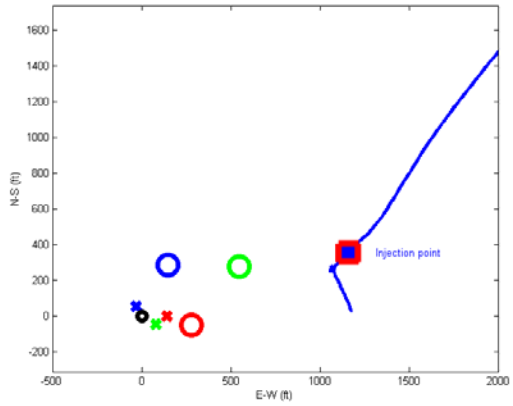

Figure 8 A map view of three relatively located Slave events (crosses) and directly located events (circles). The Master event location is represented as a black circle at the origin of coordinate system and well trajectory is shown as a blue line, red square is injection point for Stage 6. Color-coding corresponds to the relocation of Slave events, e.g. red cross represents new location of the red circle.

Conclusions

We have developed a new methodology to detect weak signal of microseismic events by cross-correlation with waveforms of a strong event (called a Master event). This allowed us to detect and relatively locate a number of weak events triggered by hydraulic fracturing on a surface monitoring array.

Acknowledgemetns

We are grateful to Peter Duncan, Tomas Fischer, Steven Gibbons, Michael H. Grealy, BJ Hulsey, Christine Lunsford, Julia Kurpan and Phil Rawlins for fruitful advice and stimulating discussions.

EDITED REFERENCES

Note: This reference list is a copy-edited version of the reference list submitted by the author. Reference lists for the 2008 SEG Technical Program Expanded Abstracts have been copy edited so that references provided with the online metadata for each paper will achieve a high degree of linking to cited sources that appear on the Web.

REFERENCES

Eisner, L., T. Fischer, and J. Le Calvez, 2006, Detection of repeated hydraulic fracturing (out-of-zone growth) by microseismic monitoring: The Leading Edge, **25**, 547–554.

Gibbons, S. J., and F. Ringdal, 2006, The detection of low magnitude seismic events using array-based waveform correlation: Geophysical Journal International, **165**, 149–166.

———2007, The detection and location of low-magnitude earthquakes in northern Norway using multichannel waveform correlation at regional distances: Physics of the Earth and Planetary Interiors, **160**, 285–309.

Hanafy, S. M., W. Cao, K. McCarter, and G. T. Schuster, 2007, Locating trapped miners using time-reversal mirrors: Utah Tomography and Modeling/Migration Development Project Annual Report, 11–24.

Lakings, J. D., P. M. Duncan, C. Neale, and T. Theiner, 2005, Surface-based microseismic monitoring of a hydraulic fracture well stimulation in the Barnett shale: 75th Annual International Meeting, SEG, Expanded Abstracts, 605–608.

Rutledge, J. T., and W. S. Phillips, 2003, Hydraulic stimulation of natural fractures as revealed by induced microearthquakes, Carthage Cotton Valley gas field, east Texas: Geophysics, **68**, 441–452.

Yilmax, O., 1987, Seismic data processing investigations in geophysics: SEG.